Hindawi
Wireless Communications and Mobile Computing
Volume 2023, Article ID 4352786, 8 pages
https://doi.org/10.1155/2023/4352786

*Research Article*

# Multiband Cooperative Spectrum Sensing Meets Vehicular Network: Relying on CNN-LSTM Approach

**Lingyun Lu,[1] Xiang Li,[2] Guizhu Wang,[3] and Wei Ni[4]**

[1]*School of Software Engineering, Beijing Jiaotong University, Beijing 100091, China*
[2]*School of Computer and Information Technology, Beijing Jiaotong University, Beijing 100091, China*
[3]*Rizhao Big Data Development Bureau, Rizhao 276826, China*
[4]*The Commonwealth Scientific and Industrial Research Organisation, Sydney, Australia*

Correspondence should be addressed to Xiang Li; 19112017@bjtu.edu.cn

Received 29 November 2022; Revised 6 March 2023; Accepted 2 June 2023; Published 16 June 2023

Academic Editor: Meng Li



A vehicular network is expected to empower all aspects of the intelligent transportation system (ITS) and aim at improving road safety and traffic efficiency. In view of the fact that spectrum scarcity becomes more severe owing to the increasing number of connected vehicles, implying spectrum sensing technology in vehicular network, i.e., cognitive vehicular network, has emerged as a promising solution to provide opportunistic usage of licensed spectrum. However, some unique features of vehicular networks, such as high movement and dynamic topology, take on high challenges for spectrum sensing. Recently, machine learning-based approaches, especially deep learning, for spectrum sensing have attracted sufficient interest. In this work, we investigate a learning-based cooperative spectrum sensing (CSS) approach for multiband spectrum sensing in the cognitive vehicular network. Specifically, we integrate two powerful deep learning models, i.e., the convolutional neural network (CNN) to exploit the features from sensing data, and the long-short-term memory (LSTM) network is then utilized to extract temporal correlations given input as the generated features by the CNN structure. Instead of the predefined decision threshold typically set in conventional approaches, our proposed approach could eliminate the impact of impertinent threshold value setting. Extensive simulations have been conducted to evaluate the effectiveness of the proposed method in achieving satisfactory spectrum sensing performance, particularly in terms of higher detection accuracy, robustness in low signal-to-noise ratio (SNR) environments, and a significant reduction in spectrum sensing time compared to other methods.

## 1. Introduction

The unprecedented development of intelligent transportation system (ITS) and various vehicular applications magnifies the scarcity of available spectrum resources. Meanwhile, in light of the fact that the licensed spectrum is usually not fully utilized, cognitive radio (CR) has been recognized as a promising solution to improve spectrum utilization. As the core technique of CR, spectrum sensing (SS) plays a key role in identifying the spectrum occupancy state associated with licensed users (i.e., primary users and PUs). The unlicensed users, called secondary users (SUs), are allowed to opportunistically access the spectrum that is not occupied by its incumbent PU. During the past decades, a variety of research works on effective spectrum sensing have been fully studied in conventional wireless network. Nevertheless, it is still in the development stage to implement spectrum sensing in vehicular network due to a series of challenges brought on by the high-speed movement of vehicles, such as the fluctuation of wireless communication channels, the dynamics of the network topology, and the diverse environments where the vehicular network is located [1].

Conventional spectrum sensing schemes typically rely on well-designed test statistics based on received sensing signals and then compare them with a predefined threshold to check the spectrum availability. According to the requirement for a priori information about PU's signal (such as modulation type and grade, pulse shape, and frame format) and noise (e.g., channel model and power), those spectrum sensing schemes can be classified into three categories:

nonblind, semiblind, and completely blind. The nonblind spectrum sensing schemes require both accurate statistical models of the PU's signal and noise. For example, derived from the log-likelihood ratio (LLR) detection, the estimator-correlator (E-C) detection has been proved to achieve the theoretical optimum [2] and provide perfect knowledge of both PU signals and noises. Accordingly, Gardner designed cyclostationary detection by exploiting the cyclostationarity attributes of received signals, which can differentiate noise from primary users' signals [3]. Similarly, matched filtering (MF) detection was proposed in [4] if certain PU signal information is known, but it requires perfect timing and synchronization which increases the calculation complexity. Among the semiblind schemes, energy detection (ED) is the most common way [5] which only needs the knowledge of noise power and thus has low implementation complexity. However, the performance of energy detection practically faces challenges due to the existence of noise uncertainty, and it fails to work when the signal-to-noise ratio (SNR) falls below some threshold, which is commonly known as the SNR-wall problem. To get rid of any a priori knowledge on PU signal or noise power, eigenvalue-based detection [6] and covariance matrix-based detection [7] are two preferred approaches with respect to the totally blind schemes. Although they reveal robustness against low SNR condition and noise uncertainty, extra computational cost is needed for computing the statistical covariance matrix and substantial eigenvalues. In conclusion, these works are mainly based on test statistic design with empirically statistical modeling, which might not perform favorably in a real-time-varying vehicular network, thus resulting in significant performance degradation.

In contrast to conventional model-driven methods, by exploiting the test statistics of received sensing signals, motivated by recent trends in machine learning (ML) applied to wireless communication which has proved great success, comprehensive learning-based applications for spectrum sensing have been advocated. The spectrum sensing process is equivalent to a binary classification problem in the context of ML. There are various studies related to ML models for spectrum sensing, which include but are not limited to the hidden Markov model (HMM), decision tree (DT), linear autoregressive model, support vector machine (SVM), and Gaussian mixture model (GMM). Specifically, deep learning (DL) presents an outstanding performance in many areas because of its powerful ability to extract complex features in a data-driven way. For example, to benefit from the powerful capability of convolutional neural network (CNN) in extracting features from matrix-shaped data, Liu et al. [8] dealed with the sample covariance matrix as the CNN input and proposed a covariance matrix-aware CNN (CM-CNN) method which significantly outperforms other spectrum sensing methods. Chen et al. [9] utilized the short-time Fourier transform (STFT) to obtain rich information by time-frequency analyses, and then a STFT-CNN spectrum sensing model was designed to extract the features of the time-frequency matrix and further improve the sensing accuracy under low SNR. Besides, to address the problem of labeled data shortage as vehicular network changes over time, Xie et al. [10] developed an unsupervised deep learning-based spectrum sensing method (UDSS), which established the variational autoencoder with the Gaussian mixture model that achieves close performance compared with the supervised learning-based benchmarks. Several works with a generative adversarial network (GAN) have been proposed to generate synthetic data for training when the number of training samples is insufficient and the spectrum sensing model can be retrained in a new environment, thus enhancing its adaptability [11, 12].

In practical wireless communication, the quality of PUs' signal detected at SUs is easily degraded; even SUs cannot receive PUs' signal which is known as the hidden node problem. Besides, the sensing reliability of individual SUs is susceptible to errors, leading to incorrect prediction of the occupancy state of the licensed spectrum. To overcome these issues, cooperative spectrum sensing (CSS) is viewed as a better solution, where all SUs exchange their sensing information with a fusion center (FC) for global decision-making. The FC might be part of the network infrastructure such as the wireless access point or one of the SUs. It combines the sensing information from all participating SUs, follows some fusion rules, analyzes the spectrum availability, and then feedbacks the prediction result of the spectrum occupancy state.

Despite the aforementioned studies, especially the usage of DL, which have shown extreme success in solving spectrum sensing problem, there are still many challenges that need to be solved urgently. One weakness of most spectrum sensing approaches is that they seldom consider the temporal correlation of received signals across multiple sensing periods. It has been reflected that when a PU turns from the silent state to the transmission state, it will probably stay in the transmission state for multiple sensing periods and vice versa [13, 14], thus the PU's pattern should be fully harnessed to improve the spectrum sensing performance. In addition, it is of vital importance to perform sensing over a wide frequency range, i.e., multiband spectrum sensing, whereas existing studies usually perform spectrum sensing over a single band. Intuitively, this problem can be addressed by converting it into a series of single-band spectrum sensing. However, implementing spectrum sensing in each subband independently may ignore the correlation between subbands.

In this paper, we consider multiband spectrum sensing utilizing deep learning models in a cooperative way. Specifically, considering that the covariance matrix of received signals has been inherent as the scope of interest input features in relative researches, we first propose a covariance matrix-aware CNN model, and then a LSTM shows a powerful capability to capture the temporal features from time series data. It is worth highlighting that the proposed detection does not require any additional information about the primary signal or noise density when deployed online. Through extensive simulation and comparison, the advantages of the proposed detection method are verified compared with traditional spectrum sensing methods. In addition, the effects of different false alarm probabilities, different sampling lengths, and different modulation types on the detection performance of the proposed model are also explored.

The remainder of this paper is organized as follows. Section 2 presents the system model. In Section 3, our proposed multiband cooperative spectrum sensing approach is described in detail. Extensive simulations are discussed in Section 4, followed by conclusions in Section 5.

## 2. System Model

As shown in Figure 1, we consider a multiband cognitive vehicular network consisting of $M$, PUs, and $K$ cognitive vehicle users (CVU). The system spectrum is divided equally into $Q$ nonoverlapping subbands. The set of PUs, CVUs, and available subbands is collected as $\mathcal{M}$, $\mathcal{K}$, and $\mathcal{Q}$, respectively. For convenience, we suppose each PU randomly selects a fixed number of $Q_m$ consecutive subbands that can meet its communication requirement. Furthermore, the power leakage effect is considered, which means the occupied subbands with PU's signal may influence the adjacent idle subband [15], and the proportion of power leakage is set to $\eta$.

According to subband occupancy, an arbitrary subband $q$ can be categorized into three cases: occupied by PU ($q \in \mathcal{Q}_o$), fully vacant ($q \in \mathcal{Q}_v$), and vacant but influenced by power leakage ($q \in \mathcal{Q}_{vp}$). In this paper, we consider the subband-occupied case as $\mathcal{H}_1$ hypothesis, and the other two cases are viewed as $\mathcal{H}_0$ hypothesis. An example of the possible spectrum occupancy state of two PUs is shown in Figure 2.

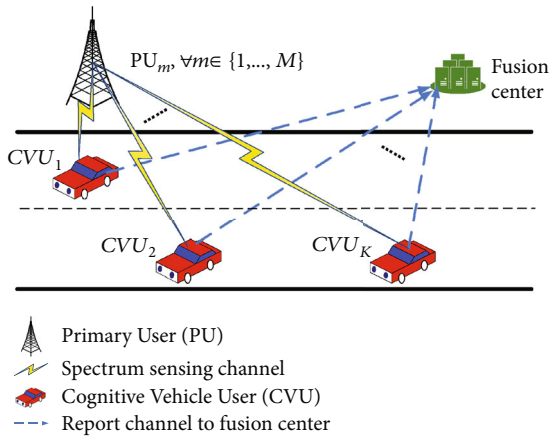


Figure 1: The cooperative spectrum sensing system for the cognitive vehicular network.

$$y_{k,n}(q) = \begin{cases} \sum_{m=1}^{M} \alpha_q^m \sqrt{P_{\mathrm{PU}}} h_{m,k}(q) s_{m,n} + w_n(q), & \text{case1} : q \in \mathcal{Q}_o, \\ \sqrt{\eta} \sum_{m=1}^{M} \alpha_{q_-}^m \sqrt{P_{\mathrm{PU}}} h_{m,k}(q_-) s_{m,n} + \sqrt{\eta} \sum_{m=1}^{M} \alpha_{q_+}^m \sqrt{P_{\mathrm{PU}}} h_{m,k}(q_+) s_{m,n} + w_n(q), & \text{case2} : q \in \mathcal{Q}_{vp} \\ w_n(q), & \text{case3} : q \in \mathcal{Q}_v. \end{cases} \quad (1)$$

During a spectrum sensing period, each CVU aims to perform spectrum sensing to decide vacant subbands for access through capturing $N$ signal sampling on each subband. Therefore, the $n$th received a signal sample of the $k$ th CVU on the $q$th subband can be represented as equation (1). Here, $w_n(q)$ is the additive noise on the subband $q$ following the zero mean circularly symmetric complex Gaussian (CSCG) distribution with variance $\sigma_\omega^2$. The binary indicator $\alpha_q^m \in \{0, 1\}$ means that the $m$th PU is inactive or active on the subband $q$, and it is limited that $\sum_{m=1}^{M} \alpha_q^m \leq 1$ indicating only one PU can access to individual subband in each sensing period to avoid mutual interference. The PUs' transmit power is fixed as $\sqrt{P_{\mathrm{PU}}}$, and $s_{m,n}$ is the transmit symbol of the $m$th PU at sampling time $n$. The variables $q_-$ and $q_+$ denote two adjacent subbands of subband $q$, respectively. $h_{m,k}(q)$ denotes the channel gain from the $m$th PU to the $k$th CVU on a subband $q$ modeled as

$$h_{m,k}(q) = \sqrt{\mathrm{PL}\left(\left\| c_m^{PU} - c_k^{CVU} \right\|_2\right)} \cdot \nu_{m,k}. \quad (2)$$

Here $c_m^{PU}$ and $c_k^{CVU}$ are the two-dimensional coordinates of PUs and CVUs, respectively. The operation $\|\cdot\|_2$ is to evaluate the Euclidean distance, and $\mathrm{PL}(d) = d^{-\beta}$ is the power loss in the propagation with regard to distance $d$ and path-loss exponent $\beta$. $\nu_{m,k}$ represents the fading coefficient, and in this paper, it is assumed that the transmitted signal experiences a quasi-static channel. Therefore, the received sampling signal matrix of CVU $k$ can be represented as $\mathbf{Y}_k = [\mathbf{y}_k(1) \cdots \mathbf{y}_k(q) \cdots \mathbf{y}_k(Q)]^T$, i.e.,

$$\mathbf{Y}_k = \begin{cases} y_{k,1}(1) & \cdots & y_{k,n}(1) & \cdots & y_{k,N}(1), \\ \vdots & \ddots & \vdots & \ddots & \vdots \\ y_{k,1}(q) & \cdots & y_{k,n}(q) & \cdots & y_{k,N}(q), \\ \vdots & \ddots & \vdots & \ddots & \vdots \\ y_{k,1}(Q) & \cdots & y_{k,n}(Q) & \cdots & y_{k,N}(Q). \end{cases} \quad (3)$$

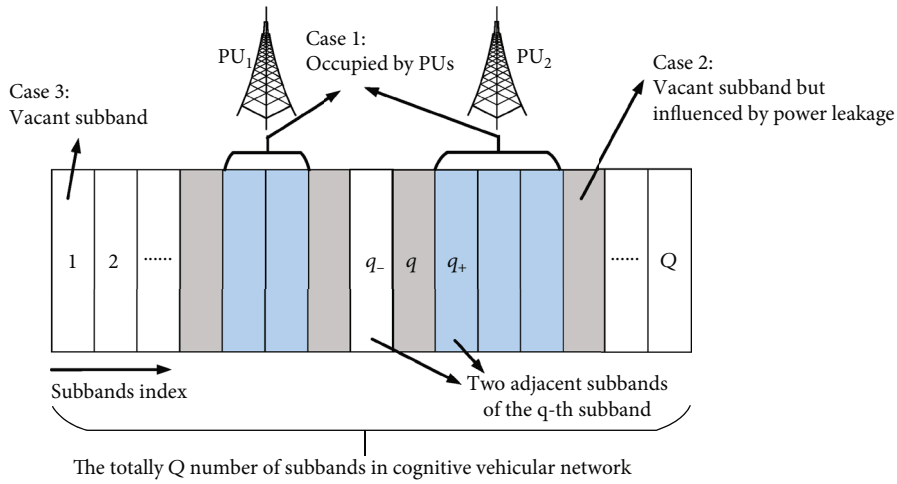


Figure 2: The illustration of the subband occupancy state of two PU systems.

## 3. The Proposed Multiband Cooperative Spectrum Sensing Approach Based on CNN-LSTM

The purpose of the spectrum sensing problem in the context of deep learning is equivalent to constructing a classifier, which can correctly map the collected $K$ received signal vectors $\mathbf{Y}_k, \forall k \in \mathcal{K}$ to the subband occupancy state. In this section, we next illustrate the details of the proposed multiband cooperative spectrum sensing algorithm.

*3.1. Data Preprocessing.* Instead of utilizing the originally received sampling signal matrix for following spectrum sensing decision, we adopt sample covariance matrix transform, i.e., calculating the covariance matrix of each sample $\mathbf{y}_k(q), \forall q \in \mathcal{Q}$ on all subbands denoted as $\mathbf{R}_k(q)$.

$$\mathbf{R}_k(q) = \frac{1}{N}\mathbf{y}_k(q)\mathbf{y}_k^H(q). \tag{4}$$

Then, we concatenate the multiband covariance matrices as the collected feature matrix locally of the $k$th CVU, i.e.,

$$\mathbf{R}_k = \begin{bmatrix} \mathbf{R}_k(1) \\ \vdots \\ \mathbf{R}_k(q) \\ \vdots \\ \mathbf{R}_k(Q) \end{bmatrix}. \tag{5}$$

At each sensing period, the fusion center can collect all $K$ local feature matrices $\{\mathbf{R}_k, \forall k \in \mathcal{K}\}$ and put them together as a feature matrix globally $\mathbf{X} = [\mathbf{R}_1 \cdots \mathbf{R}_k \cdots \mathbf{R}_K]$, which is viewed as the input of the learning module to perform multiband cooperative spectrum sensing.

$$\mathbf{X} = \begin{pmatrix} \mathbf{R}_1(1) & \cdots \mathbf{R}_k(1) & \cdots & \mathbf{R}_K(1) \\ \mathbf{R}_1(2) & \cdots \mathbf{R}_k(2) & \cdots & \mathbf{R}_K(2) \\ \vdots & \vdots & \vdots & \\ \mathbf{R}_1(Q) & \cdots \mathbf{R}_k(Q) & \cdots & \mathbf{R}_K(Q) \end{pmatrix}. \tag{6}$$

It is required to collect enough labeled training data firstly for execution following the deep learning approach. We first collect sensing data over $T$ consecutive sensing periods, where each data consists of the global feature matrix and corresponding subband occupancy, i.e., $(\mathbf{X}^{(1)}, \mathbf{a}^{(1)}), \cdots, (\mathbf{X}^{(t)}, \mathbf{a}^{(t)}), \cdots, (\mathbf{X}^{(T)}, \mathbf{a}^{(T)})$. The subbands occupancy $\mathbf{a}^{(t)}$ is a vector with a length of $Q$, in which each element is 1 or 0 indicating the corresponding subband is or not be occupied. Furthermore, we rearrange those $T$ number of consecutive sensing data in order to excavate the inherent pattern of PUs. Specifically, a sequence of $\lambda$ length sensing data is combined, and we obtain the required training dataset $\mathbf{D} = (\mathbf{d}_1, \mathbf{b}_1), \cdots, (\mathbf{d}_u, \mathbf{b}_u), \cdots, (\mathbf{d}_U, \mathbf{b}_U)$, where $d_u = [\mathbf{X}^{(u)}, \mathbf{X}^{(u+1)}, \cdots, \mathbf{X}^{(u+\lambda-1)}]$ and $\mathbf{b}_u = \mathbf{a}^{(u+\lambda-1)}$. It means that the built classifier can predict current subband occupancy via both the current sensing feature vector and previous $\lambda - 1$ sensing feature vectors. The training dataset $\mathbf{D}$ for the following network training is built, which has $U = T - \lambda + 1$ number of training samples. The procedure of data preprocessing above is illustrated in Figure 3.

*3.2. Network Structure and Learning Process.* The network structure of the proposed learning approach is shown in Figure 4, which is inspired by [16]. The training sample $d_u$ is in complex value and thus can be witnessed as a series of two-layer images with a length of $\lambda$. We first sequentially input the training sample into the CNN module which consists of two convolutional layers. Two parallel structures containing multiple convolution layers and max-pooling layers intake and process the observation of present and historical sensing periods. After the convolution-pooling structure, the outputs of the two parallel structures are flattened

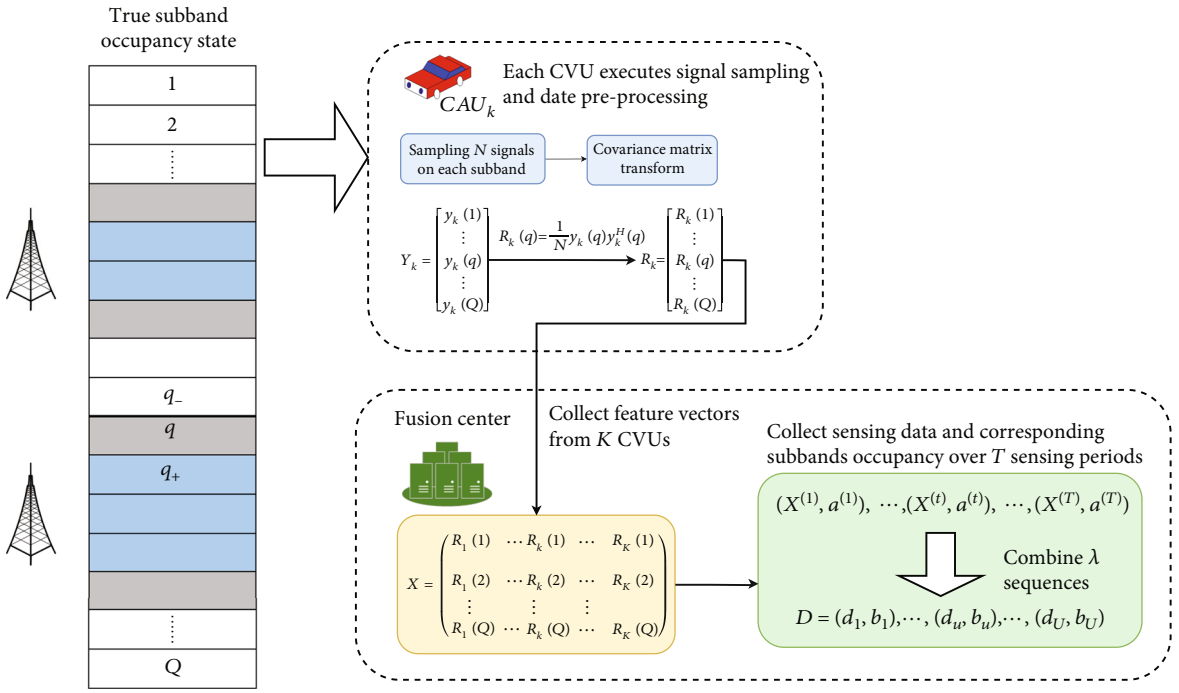


FIGURE 3: The procedure of data preprocessing.

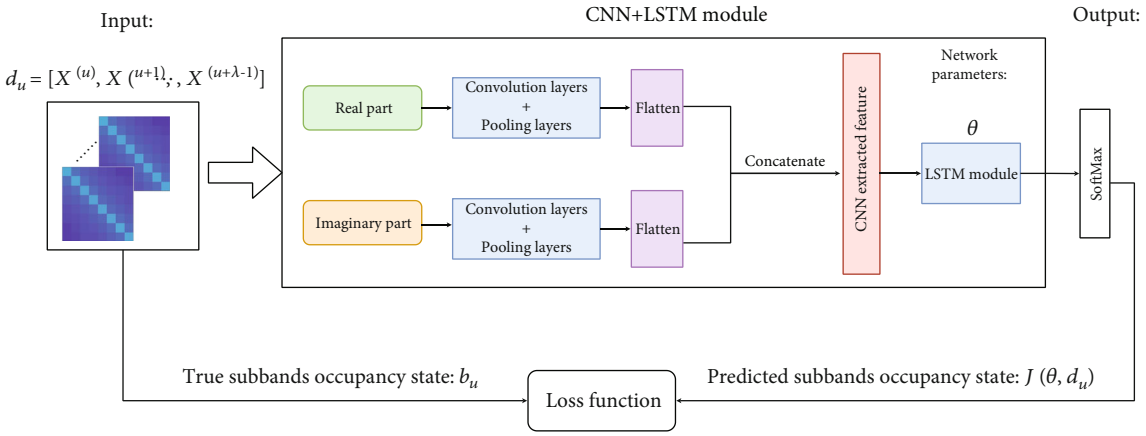


FIGURE 4: Network architecture of the proposed learning approach.

into two vectors and then concatenated. The CNN-extracted feature is viewed as the input into the following LSTM modules, which are responsible to exploit the time-dynamic correlations concealed in the series of sensing periods. At last, the output of the last LSTM cell is catenated with a dense layer to stand for the belief that the input corresponds to predicted subband occupancy.

After the formulation of the training input and the network structure, the next process is to design the loss function to train our proposed classifier. Given a training sample $<\mathbf{d}_u, \mathbf{b}_u>$, let $\mathcal{J}(\mathbf{d}_u; \boldsymbol{\theta})$ the prediction subband occupancy vector from the classifier, $\boldsymbol{\theta}$ be the classifier parameters. The categorical cross-entropy loss function, as formulated in equation (7), is employed to measure the difference between prediction value $\mathcal{J}(\mathbf{d}_u; \boldsymbol{\theta})$ and actual subband occupancy $\mathbf{b}_u$.

$$\mathcal{L}(\mathbf{d}_u, \mathbf{b}_u; \boldsymbol{\theta}) = -\sum_{q=1}^{Q} \mathbf{b}_u^{(q)} \log \mathbf{J}(\mathbf{d}_u; \boldsymbol{\theta})^{(q)} \tag{7}$$

Here, the $\mathbf{J}(\mathbf{d}_u; \boldsymbol{\theta})^{(q)}$ and $\mathbf{b}_u^{(q)}$ is the $q$th element of the actual/prediction subband occupancy vectors. In this way, the training loss on the collected training dataset can be denoted as $1/U \sum_u \mathcal{L}(\mathbf{d}_u, \mathbf{b}_u; \boldsymbol{\theta})$.

To minimize the loss value, the stochastic gradient descent (SGD) method and adaptive moment estimation (Adam) optimizer are adopted. The trained classifier can be evoked to recognize the subband occupancy pattern based on the matrix collected by all CAUs. In general, the training module should be activated when the network is initialized

Table 1: Network parameters of the proposed approach.

| Network parameters | Value |
|---|---|
| Filters per conv layer | 6 |
| Filter size | 16 |
| Cells per LSTM layer | 20 |
| Neurons per flattened layer | 128 |
| Optimizer | Adam |
| Learning rate | 0.003 |
| Batch size | 200 |

and periodically configured to catch up with the changing radio environment.

## 4. Numerical Analysis

*4.1. Dataset Prerequisite.* The PU signals are retrieved from the open-source RadioML2018.01a dataset [17], which includes 24 kinds of typically digital and analog modulated signals. For each class of modulation type, it contains 26 levels of SNR ranging from -20 to 30 dB with intervals of 2 dB. Each ⟨modulation, SNR⟩ pair is composed of 4096 examples and has a length of 1024 in-phase and quadrature (I/Q) complex-value per example. For simplicity, in this study, we limit the datasets to negative SNR, and seven linear modulations are simulated: BPSK, QPSK, 8PSK, 8QAM, 16QAM, 32QAM, and 64QAM. The entire dataset is partitioned into three halves for training, validating, and testing with a commonly used split ratio of 7 : 2 : 1.

*4.2. Simulation Parameters.* We conduct numerical experiments to corroborate the performance of the proposed method in a multiband cognitive vehicular network with $M = 3$ PUs using $Q = 16$ subbands for communication. The 3 PUs occupy 2, 3, and 4 consecutive subbands, respectively. On the channel model, Rayleigh fading is assumed with path-loss exponent $\alpha = 4$, the fading component $\nu = 1$. For the convenience of analysis, we set $P(H_1) = P(H_0) = 0.5$ about the PU activity pattern. During the network training process, we define 100 SGD iterations as an epoch, and after each epoch, we check the classification accuracy on the validation set and save the network parameters if the present sensing accuracy on the validation set is higher than that corresponding to the previous epochs. The network parameters determined through extensive cross-validation are detailed in Table 1. The Pytorch-based simulations are implemented on a computer with a CPU (Intel(R) Xeon(R) Gold 6134 M) and a GPU (NVIDIA Quadro P5000).

*4.3. Results Evaluation.* In this section, extensive simulation results are provided to demonstrate the performance superiority of the proposed approach. Also, the impact of key parameters such as SNR level and modulation scheme is investigated. For comparison, the benchmark methods include the traditional rule-based cooperative spectrum sensing methods, i.e., AND rule and the OR rule, two typically test-statistic methods such as energy detection (ED) [5], maximum-minimum eigenvalue (MME) [6], and another learning method of SVM, $K$-means, and covariance matrix CNN (CM-CNN) [8]. Note that all the baseline methods are introduced for narrowband spectrum sensing, and thus all the sensing results of them are obtained in each

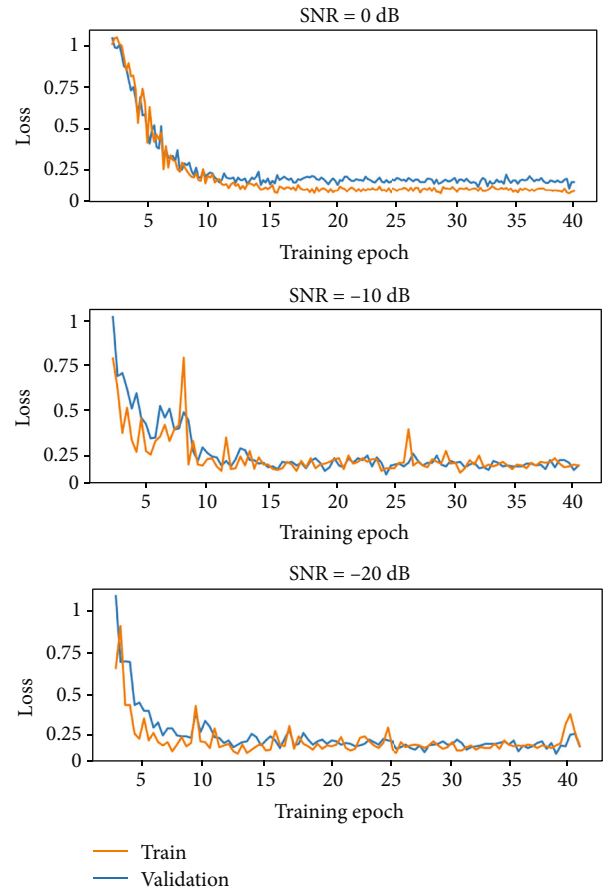


Figure 5: The loss value with training epoch iteration.

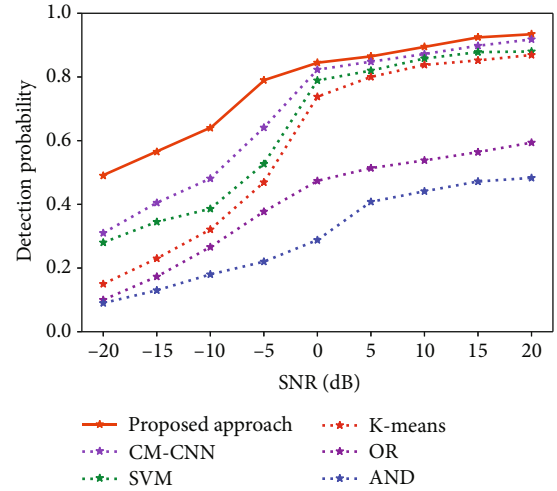


Figure 6: The detection probability of different methods.

Table 2: Complexity comparison of different spectrum sensing methods on offline training phase.

| Metrics | Proposed | CM-CNN | SVM | $K$-means |
|---|---|---|---|---|
| FLOPs ($\times 10^7$) | 1.79 | 1.21 | 0.71 | 0.027 |
| Parameters ($\times 10^6$) | 0.169 | 0.141 | 0.092 | 0.047 |
| Training time (seconds) | 170.5 | 138.01 | 63.2 | 40.9 |

Table 3: The prediction time (seconds) of different spectrum sensing methods in the online testing phase.

| Proposed method | CM-CNN | SVM | $K$-means |
|---|---|---|---|
| 0.057 | 0.083 | 0.12 | 0.07 |

subband separately. Each point in the simulation results is obtained by averaging 100 Monte Carlo realizations.

*4.3.1. Loss function's Convergence with SNR Level.* First, we evaluate the loss function's convergence behavior under different SNR levels. As shown in Figure 5, with the epoch of the model training, both training loss and validation loss are decreasing. In high SNR scenarios, the difference in extracted features from spectrum sensing data between idel subbands and occupied subbands is large, and therefore, the loss function shows quick convergence. With the decline of SNR, i.e., the wireless channel condition becomes worse; the inapparent difference in the subband state makes the classification task more difficult. The loss curve of the training process needs more iterative rounds to obtain statistical results. In addition, the loss value of the proposed approach is reduced smoothly in the training process and shows its superiority.

*4.3.2. Spectrum Sensing Performance.* The performance of the spectrum sensing algorithm is mainly evaluated by the detection probability. A higher detection probability signifies a better capability to protect PUs.Figure 6 shows the spectrum detection probability of the proposed approach and other compared methods under different SNR conditions. We can see that even under the condition of low SNRs, the detection probability of the proposed approach is still better than the others. Because the LSTM structure learns the time characteristics of historical sensing data, it obtains higher detection accuracy. It is depicted that the proposed approach can achieve the highest detection probability, and the detection probability of CM-CNN is slightly lower, closely approaching that of the proposed method. The SVM scheme is in the middle of performance. The detection probability of $K$-means is lower since it is an unsupervised learning diagram. The detection probability of the rule-based scheme is the lowest one due to the high difficulty of a full vote among all the SUs. It is also interesting that for the fusion rule, the detection probability of the AND-rule is a little lower than the OR-rule-based scheme. From these simulation results, we can see that the proposed classifier generally exhibits relatively superior performance and achieves the best performance among them.

*4.3.3. Complexity Comparison.* Finally, the specific complexity of different methods is compared. When analyzing the complexity of different methods, we consider three metrics in the offline training phase, namely, the required number of floating point operations (FLOPs), the total number of parameters, and the offline training time. The classifier training has usually been executed once in practice; therefore, we only evaluate the prediction delay in the online testing phase. Two tables (Tables 2 and 3) have been simulated to verify the superiority of the proposed method over others.

As a comparison, the proposed method demands the highest offline training duration among all the classifiers, and the additional FLOPs overhead is higher than other methods. For the classifier built on neural network methods, i.e., the proposed method and the CM-CNN method, they require a larger parameter number because of the cascaded structure of the neural network. Both the training duration and prediction delay for the $K$-means are founded to be normal. The proposed method shows the most rapid spectrum occupancy prediction. In addition, the SVM suffers from a very high prediction delay. It can be viewed that the proposed spectrum sensing approach can predict the spectrum state by mining the internal correlation of historical data, so the overall sensing time is greatly shortened. Another observation is reflected intuitively that with more sufficient training samples, it takes more effort to train the classifier to a satisfactory results.

## 5. Conclusion

In this work, we have studied the problem of multiband spectrum sensing in a cognitive vehicular network and developed a cooperative spectrum sensing algorithm based on the covariance matrix-aware CNN-LSTM. The proposed method can effectively learn the underlying dependence features across adjacent subbands and consecutive sensing periods to improve spectrum sensing performance. Numerical results demonstrated that the proposed method has a substantial performance advantage over other existing methods under noise uncertainty.

## Data Availability

The data used in the simulation are retrieved from the open-source RadioML2018.01a dataset.

## Conflicts of Interest

The authors declare that they have no conflicts of interest.

## Acknowledgments

This project is supported by the Fundamental Research Funds for the Central Universities (2021CZ102).

## References

[1] J. Li and B. J. Hu, "Quantized cooperative spectrum sensing in bandwidth-constrained cognitive V2X based on deep learning," *Electronics*, vol. 10, no. 11, p. 1315, 2021.

[2] R. D. Hippenstiel, *Detection Theory: Applications and Digital Signal Processing, [M.S. Thesis]*, CRC Press, 2017.

[3] W. A. Gardner, "Exploitation of spectral redundancy in cyclostationary signals," *IEEE Signal Processing Magazine*, vol. 8, no. 2, pp. 14–36, 1991.

[4] X. Zhang, R. Chai, and F. Gao, "Matched filter based spectrum sensing and power level detection for cognitive radio network," in *2014 IEEE Global Conference on Signal and Information Processing (GlobalSIP)*, pp. 1267–1270, Atlanta, GA, USA, 2014.

[5] F. F. Digham, M. -S. Alouini, and M. K. Simon, "On the energy detection of unknown signals over fading channels," *IEEE Transactions on Communications*, vol. 55, no. 1, pp. 21–24, 2007.

[6] Y. Zeng, C. L. Koh, and Y. C. Liang, "Maximum eigenvalue detection: theory and application," in *2008 IEEE international conference on communications*, pp. 4160–4164, Beijing, China, 2008.

[7] Y. Zeng and Y. C. Liang, "Spectrum-sensing algorithms for cognitive radio based on statistical covariances," *IEEE Transactions on Vehicular Technology*, vol. 58, no. 4, pp. 1804–1815, 2009.

[8] C. Liu, J. Wang, X. Liu, and Y.-C. Liang, "Deep CM-CNN for spectrum sensing in cognitive radio," *IEEE Journal on Selected Areas in Communications*, vol. 37, no. 10, pp. 2306–2321, 2019.

[9] Z. Chen, Y.-Q. Xu, H. Wang, and D. Guo, "Deep STFT-CNN for spectrum sensing in cognitive radio," *IEEE Communications Letters*, vol. 25, no. 3, pp. 864–868, 2021.

[10] J. Xie, J. Fang, C. Liu, and L. Yang, "Unsupervised deep spectrum sensing: a variational auto-encoder based approach," *IEEE Transactions on Vehicular Technology*, vol. 69, no. 5, pp. 5307–5319, 2020.

[11] K. Davaslioglu and Y. E. Sagduyu, "Generative adversarial learning for spectrum sensing," in *2018 IEEE international conference on communications (ICC)*, pp. 1–6, Kansas City, MO, USA, 2018.

[12] C. Wang, Y. Xu, Z. Chen, J. Tian, P. Cheng, and M. Li, "Adversarial learning-based spectrum sensing in cognitive radio," *IEEE Wireless Communications Letters*, vol. 11, no. 3, pp. 498–502, 2022.

[13] J. Xie, J. Fang, C. Liu, and X. Li, "Deep learning-based spectrum sensing in cognitive radio: a CNN-LSTM approach," *IEEE Communications Letters*, vol. 24, no. 10, pp. 2196–2200, 2020.

[14] J. Gao, X. Yi, C. Zhong, X. Chen, and Z. Zhang, "Deep learning for spectrum sensing," *IEEE Wireless Communications Letters*, vol. 8, no. 6, pp. 1727–1730, 2019.

[15] J. Zhang, Z.-Q. He, H. Rui, and X. Xu, "Multiband joint spectrum sensing via covariance matrix-aware convolutional neural network," *IEEE Communications Letters*, vol. 26, no. 7, pp. 1578–1582, 2022.

[16] N. E. West and T. O'shea, "Deep architectures for modulation recognition," in *2017 IEEE International Symposium on Dynamic Spectrum Access Networks (DySPAN)*, pp. 1–6, Baltimore, MD, USA, 2017.

[17] T. J. O'Shea, T. Roy, and T. C. Clancy, "Over-the-air deep learning based radio signal classification," *IEEE Journal of Selected Topics in Signal Processing*, vol. 12, no. 1, pp. 168–179, 2018.